RSC Advances

PAPER

View Article Online
View Journal | View Issue



Cite this: *RSC Adv.*, 2025, **15**, 199

# Dual-recognition driven sensing platform based on a BSA-Cu NP nanozyme combined with smartphone-assistance for fluorometric/colorimetric monitoring of dopamine†

Da-Qian Feng, Shaofei Wang, Zhendi Yu, Wenfeng Zhang and Guoliang Liu *

Developing a highly sensitive approach for neurotransmitter analysis is of vital significance due to their essential role in clinical diagnosis and treatment of disease. Herein, bovine serum albumin templated copper nanoparticles (BSA-Cu NPs) with peroxidase-mimicking activity are designed and synthesized for dopamine detection through the fluorometric/colorimetric dual-mode technique. The experimental results suggest that as-fabricated BSA-Cu NPs can strongly catalyze the decomposition of hydrogen peroxide to produce oxidized substances, accompanied by remarkable color changes of chromogenic agent 3,3′,5,5′-tetramethylbenzidine from colorless to blue, revealing peroxidase-like activities of BSA-Cu NPs. However, owing to the strong binding affinity between dopamine (DA) and BSA-Cu NPs, the catalytic activities of synthesized BSA-Cu NPs are inhibited, leading to a significant decrement of absorption peak signal. Meanwhile, the strong fluorescence of BSA-Cu NPs exhibits remarkable quenching due to photo-induced electron transfer. Besides, by integrating paper strips and smartphone software analysis, an intelligent recognition of DA is also fabricated. On the basis of these phenomena, a fluorometric/colorimetric approach based on the BSA-Cu NP nanozyme combined with smartphone-assisted analysis is constructed for detecting dopamine with a detection limit of 5 nM, and 5 nM, respectively. Moreover, the recognition of dopamine in human serum samples is also successfully realized which is verified using high performance liquid chromatography, demonstrating its promising potential in bioanalysis and clinical disease diagnosis.

Received 7th October 2024
Accepted 21st December 2024

DOI: 10.1039/d4ra07209j

rsc.li/rsc-advances



## 1. Introduction

In recent years, ultra-small molecular nanoparticles (MNPs) as promising substitutes to organic dyes and quantum dots attracted widespread interest in multiple fields such as chemical assay, biological assay, and nanomedicine due to its excellent physical and chemical properties.[1–3] Especially, fluorescent noble-metal nanoparticles also termed noble-metal nanoclusters have gained increased attention recently due to their unique properties such as ultra-small size, high biocompatibility, tunable fluorescent properties, and low toxicity.[4–7] Compared with fluorescent noble-metal nanoparticles, the synthesis of fluorescent copper nanoparticles (Cu NPs) is more economical because of the abundance and availability of synthesized materials.[8–10] However, to date, only a few experimental studies have given insight into Cu NPs, mainly focusing on fluorescent properties.[11,12] Inspired by the study where noble-metal nanoparticles emerge as artificial enzyme mimics,[13,14] it is of great significance to explore a new sensing approach based on the catalytic activity of Cu NPs.

Dopamine (DA) is an important monoamine neurotransmitter distributed in the central neural system brain tissues and body fluids of mammals.[15,16] The research suggests that normal content of DA concentration in healthy people blood ranges from 26 nM to 40 nM and below.[17] Abnormal DA levels are demonstrated to be associated with some major diseases such as Parkinson disease, schizophrenia, anorexia, and HIV infection.[18–21] Therefore, developing highly sensitive and selective approach for dopamine detection with wide linear range has important significance due to it's closely related to human physiological health. As DA is easily oxidized electrochemically at electrodes, the detection of DA by electrochemistry method is often interfered by ascorbic acid and uric acid, mainly because they have close reduction potentials to that of DA. In addition, their concentrations are 100–1000 times higher than that of DA in most biological samples.[22] Thus, the development of the method of sensitive detecting DA is still challenging.

In this contribution, based on intrinsic catalytic property of BSA-Cu NPs, as well as the strong interaction between DA and

*School of Chemistry and Chemical Engineering, Yancheng Institute of Technology, Jiangsu 224051, P. R. China. E-mail: liuguoliang199@126.com; glliu@ycit.edu.cn; Fax: +86-515-88298190; Tel: +86-515-88298190*

† Electronic supplementary information (ESI) available. See DOI: https://doi.org/10.1039/d4ra07209j

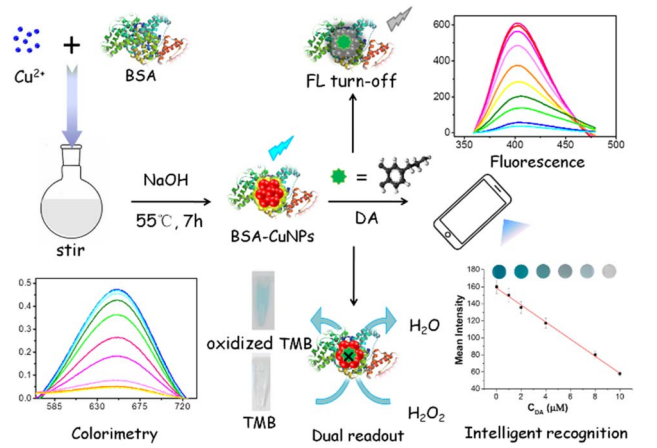


Scheme 1 Schematic illustration of fluorometric/colorimetric dual-channel sensing platform for dopamine detection based on BSA-Cu NPs nanozyme combined with smartphone-assisted analysis.

BSA-Cu NPs, as-fabricated BSA-Cu NPs with high peroxidase-like activity were prepared and applied as sensing elements to fabricate a fluorometric/colorimetric dual-channel sensor for DA detection (Scheme 1). BSA-Cu NPs can catalyze hydrogen peroxide ($H_2O_2$) to generate hydroxyl radicals (·OH), which further oxidize 3,3′,5,5′-tetramethylbenzidine (TMB) substrates to generate blue, leading to increased absorbance signal (the left lower figure in Scheme 1). Upon the addition of DA, the peroxidase-like performance of BSA-Cu NPs was significantly inhibited due to strong binding force between BSA and DA, resulting in a decreased or no color change of TMB in the presence of $H_2O_2$. Meanwhile, intrinsic fluorescent intensity of BSA-Cu NPs was incrementally restrained attribute to photo-induced electron transfer (PET) (the right upper figure in Scheme 1). Besides, by using paper strips with smartphone-assisted software analysis, an intelligent recognition of DA was also fabricated (the right lower figure in Scheme 1). Based on these experimental situations, a new label-free fluorometric/colorimetric dual-mode sensing platform combined with the smartphone-assisted analysis was developed for DA detection. Compared with the reported methods of DA detection,[23–27] the present approach possesses comparable detection limit and wider linear range. In addition, applying this sensing approach to actual human serum samples successfully with acceptable results reveals that this method possesses great potential in clinical disease diagnosis.

# 2. Experimental section

## 2.1. Materials

Bovine serum albumin (BSA), cupric sulfate ($CuSO_4$) was obtained from were from Signopharm Chemical Reagent Co., Ltd (Shanghai, China). Sodium hydroxide (NaOH), hydrochloric acid (HCl), nitric acid ($HNO_3$) and other metal salts or reagents were purchased from Shanghai Chemical Reagent Co., Ltd (Shanghai, China). All chemicals were of analytical reagent grade and used as received without further purification. The phosphate buffer solution (PBS) was used to control the acidity of the reaction system. Millipore Milli-Q ultrapure water (18.2 MΩ $cm^{-1}$) was used in all experiments.

## 2.2. Apparatus

Absorption spectra were recorded on a Shimadzu UV-2450 UV-visible spectrophotometer (Shimadzu, Japan). Fluorescence spectra were determined on Jasco FP-6500 fluorescence spectrometer (Jasco, Japan). The pH value was measured with a PHS-3C pH meter (Leici, Shanghai, China).

## 2.3. Synthesis of ultra-small size BSA-Cu NPs nanozyme

All glassware was thoroughly washed with fresh Aqua Regia ($HCl : HNO_3$ = 3 : 1 v/v), rinsed with ethanol and ultrapure water, and then dried in an oven prior to use. The Cu NPs nanozyme were synthesized in one step by the reduction of $CuSO_4$ with BSA as both reducing agent and stabilizer according to the description of previous reports with minor modifications (the left upper figure in Scheme 1).[28] Briefly, 2 mL $CuSO_4$ working solution (20.0 mM) was added into 10 mL BSA solution (15.0 mg $mL^{-1}$) under vigorous stirring for 3 minutes. After that, 1 mL NaOH solution (1.0 M) was introduced, and then the mixture was allowed to stir at 55 °C for 7 h. The reaction solution was dialyzed using 3000 Da MWCO dialysis bag in double distilled water for 48 h to remove unreacted $Cu^{2+}$ solution. At last, the concentration of the product was 3.33 mM (calculated by the molar number of copper atoms).

## 2.4. Colorimetric detection of dopamine using BSA-Cu NPs as peroxidase mimic

In a typical assay, 40 μL of Cu NPs solution (pH 7.0) was mixed with 10 μL different concentrations of analyte dopamine (0–60 μM). Then, the above Cu NPs/dopamine mixture, 80 μL TMB (15 mM) and 20 μL $H_2O_2$ (3.75 mM) were added into 400 μL of PBS (50 mM, pH 4.0). The mixture solution was incubated at 30 °C water bath for 20 min and diluted to 3 mL with 50 mM PBS (pH 4.0). The absorption spectra of the reactive solution were recorded from 500 to 800 nm with monitoring the change of absorbance intensity located at 652 nm.

## 2.5. Fluorometric detection of dopamine using BSA-Cu NPs

In a test, 300 μL of as-prepared BSA-Cu NPs working solution was diluted with PBS (50 mM, pH 7.0) and mixed with certain amount of dopamine. Various concentrations of dopamine solution was added into 3 mL of diluted BSA-Cu NPs working solution, and mixed thoroughly with gentle shaking. Final concentration of dopamine ranged from 0 to 1000 μM. The mixture was incubated at 30 °C water bath for 20 min. The fluorescence spectra were determined from 360 to 460 nm with the excitation wavelength located at 324 nm.[29–31] The slit widths of the excitation and emission were both 10 nm.

## 2.6. Smartphone-assisted analysis of dopamine using paper strips

Chromatography paper was chosen and cut into a rectangular paper strip (10 mm × 20 mm). After that, the fabricated paper

strips were soaked in the Cu NPs solutions (40 μL, pH 7.0) for 10 min. Then, TMB (0.4 mM) and $H_2O_2$ (0.025 mM) were dropped onto the test strip and incubated at room temperature for 20 min. At this moment, it exhibited a dark blue color because the test strip containing Cu NPs, $H_2O_2$ and TMB by naked eyes. Afterward, different concentrations of DA or real samples were introduced onto the paper strip. After incubating for 20 min, the color change was captured through smartphone camera. The color parameters of the image were analyzed by image software Quantity One.[32] Darkness density of each dot was picked to describe color difference among the volume data in Volume Analysis Report.

### 2.7. Detection of dopamine in real samples

The spiked-recovery experiments of colorimetric approach were performed using human serum samples obtained from healthy laboratory volunteers. The amount of dopamine in actual samples was detected by using the proposed approach described above with the standard addition method. The test process was the same as before.

## 3. Results and discussion

### 3.1. Characterization of synthesized Cu NPs

The ultra-small size water-soluble Cu NPs were synthesized by using bovine serum albumin (BSA) as a stabilizer and reducer.[33,34] The obtained BSA-Cu NPs exhibited an intense blue fluorescence under UV light. The UV-vis spectra and fluorescence emission spectrum of as-prepared BSA-Cu NPs are shown in Fig. 1A. As shown in Fig. 1A, compared with the characteristic maximum absorption peak located at 280 nm of BSA, that of synthesized BSA-Cu NPs at the same wavelength nearly appears, revealing the successful synthesis of BSA-Cu NPs indirectly, which was consistent with reported work.[28] Meanwhile, BSA-Cu NPs exhibited an emission band centered at 401 nm when it was excited at 324 nm (Fig. 1A). The quantum yield of BSA-Cu NPs in aqueous solution at room temperature was determined to be 8.0% using rhodamine B as the standard, which is higher than the reported work.[35] As shown in Fig. 1B, the size-distribution of BSA-Cu NPs exhibited good dispersibility with below 2.0 nm size. Combining all of the experimental results, fluorescence BSA-Cu NPs has been successfully synthesized.

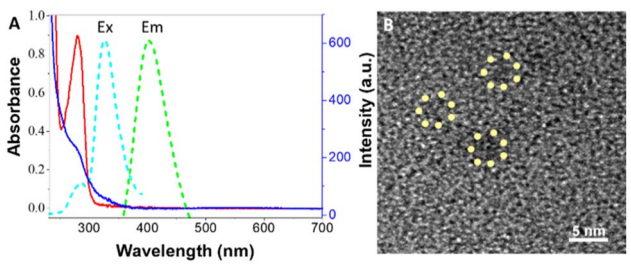


Fig. 1 (A) UV-vis absorption spectra of sole BSA (blue curve) and synthesized BSA-Cu NPs (red curve). Excitation (cyan curve) and emission spectrum (green curve) of prepared BSA-Cu NPs. (B) TEM image of synthesized BSA-Cu NPs.

### 3.2. DA detection based on fluorometric performance of BSA-Cu NPs platform

As the assay suggests that it exhibits strong fluorescence signal, BSA-Cu NPs was chosen for fluorometric detecting DA. Fig. 2A reveals that the emission spectrum of synthesized BSA-Cu NPs exhibited a maximum emission peak at approximately 401 nm upon the excitation wavelength at 324 nm (curve 1). The addition of DA can result in decrease of maximum emission intensity. Moreover, with the increasing concentrations of DA, the fluorescence intensity of the system becomes gradually quenched (curve 2–10). Thus, DA concentration is quantitatively evaluated using fluorescence intensity of BSA-Cu NPs as a sensitive response signal. The intensity of the fluorescence at 401 nm was plotted as a function of DA concentration (Fig. 2B). The linear range is from 10 nM to 60 μM with a limit of detection (LOD) for analyzing DA of 5 nM. The linear regression equation is $F_0 - F = 586.2883 - 6.5756C_{DA}$ ($R = 0.9879$). LOD is estimated by $3\sigma/k$. $\sigma$ represents the standard deviation of three blank sample and $k$ is the slope of the standard curve. Besides, horizontal stacking diagram of emission spectra clearly indicates the detailed quenching procedure of BSA-Cu NPs incubated with a series of DA (Fig. 2C). In addition, three-dimensional emission patterns exhibit distinct changes with increasing DA concentrations (Fig. 2D).

### 3.3. The mechanism of fluorometric turn-off detection of DA

Generally, fluorescent quenching phenomena is attributed to the mechanisms: photo-induced electron transfer (PET), inner filter effect (IFE), or fluorescence resonance energy transfer (FRET).[36] The fluorescent emission spectrum of BSA-Cu NPs exhibit maximum peaks located at 401 nm (Fig. 1B), the UV-vis spectra of DA molecule shows a strong absorption peak at

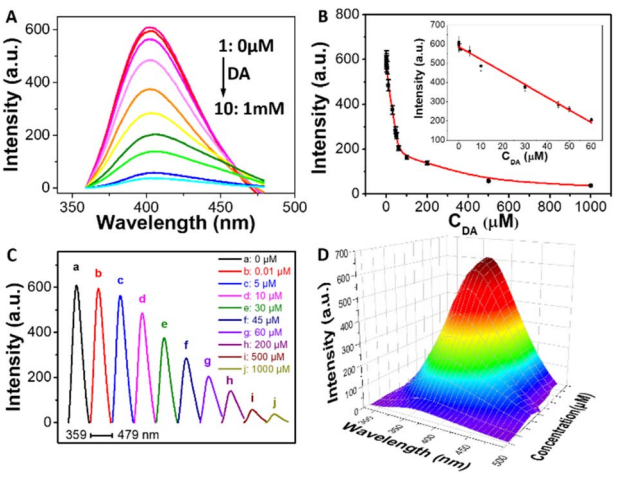


Fig. 2 (A) Fluorescence spectra of BSA-Cu NPs incubated with different amounts of DA. (B) Curve of fluorescence intensity of BSA-Cu NPs at 401 nm *versus* the concentration of DA. Inset: the linear plot for DA detection. Horizontal stacking diagram of emission spectra (C) and three-dimensional fluorescence spectrum (D) of prepared BSA-Cu NPs incubated with different concentrations of target DA. Conditions: 1 (a), BSA-Cu NPs; 2–10 (b–j): 1 + DA (μM): 0.01, 5, 10, 30, 45, 60, 200, 500, and 1000.

278 nm.[37] It doesn't appear significant overlapping between the emission peak of BSA-Cu NPs and the UV-vis absorption peak of DA, implying that fluorescence quenching caused by DA might due to PET instead of FRET or IFE.[38] To further distinguish dynamic quenching and static quenching, fluorescent lifetime of the donor molecule is also performed.[39] It turns up shortening situation from 4.52 ns to 2.65 ns, accompanying with the remarkable quenching of BSA-Cu NPs without and incubated with DA, reveals that the quenching mechanism of the system should be ascribed to dynamic quenching PET mechanism.[40] Besides, PET mechanism grant the BSA-Cu NPs probe a certain specificity for DA determination.

### 3.4. Peroxidase-mimicking activity of synthesized BSA-Cu NPs nanozyme

The peroxidase-like catalytic activity of the prepared BSA-Cu NPs is investigated. As shown in Fig. 3A, no color reaction occurs between TMB and $H_2O_2$ while TMB itself is colorless (curve 1). Upon the addition of BSA-Cu NPs, it appears a deep blue color with a significant maximum absorption peaks at 652 nm (Fig. 3A, curve 2). The distinct color change of TMB–$H_2O_2$ system occurred after introducing BSA-Cu NPs accompanied with maximum absorption peak located at 652 nm, demonstrating a peroxide-like enzyme activity of synthesized BSA-Cu NPs.[41] The principle is as follows: existed peroxidase catalyze $H_2O_2$ to generate ·OH, which further oxidize TMB to blue substrate oxidized TMB that possesses a characteristic absorption peak at 652 nm. According to previous reports, as Cu(0) and Cu(I) are both existed in the Cu NPs structure, the nature of catalytic ability of BSA-Cu NPs with peroxidase-like activity for the oxidation of TMB incubated with $H_2O_2$ can be attributed to the generation of ·OH from the decomposition of $H_2O_2$ by Cu(I) and/or Cu(0) without Cu NPs.[42] Interestingly, when a certain concentration of DA exists, the catalytic reaction of TMB–$H_2O_2$ system by BSA-Cu NPs is inhibited due to the competitive binding reaction between DA and BSA-Cu NPs, which resulting in color change from deep blue to quite light blue (curve 3 of Fig. 3A). Fig. 3B displays the time course of three different reaction systems within 10 min. Time kinetic curves exhibits the specific changing process and detailed differentiation of TMB-$H_2O_2$-Cu NPs system without and upon the addition of target DA while selecting TMB–$H_2O_2$ system as the control (Fig. 3B). These experimental results denote that prepared BSA-Cu NPs can serve as a highly efficient colorimetric sensor for dopamine detection.

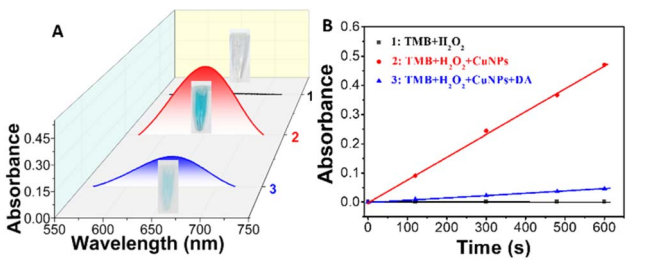


Fig. 3 Typical UV-vis absorption spectra (A) and time kinetic curves through monitoring the maximum absorbance intensity at 652 nm (B) of TMB–$H_2O_2$ system in different reaction systems. Inset is the corresponding photographs of three samples. Conditions: 1 (black curve): TMB + $H_2O_2$, 2 (red curve): TMB + $H_2O_2$ + Cu NPs, and 3 (blue curve): TMB + $H_2O_2$ + Cu NPs + 10 μM DA in PBS buffer (pH 4.0) at room temperature.

### 3.5. DA detection based on colorimetric performance of BSA-Cu NPs nanozyme platform

As a distinct color change of TMB–$H_2O_2$ system incubated with BSA-Cu NPs, the absorbance spectra was also carried out. Fig. 4A displayed that the characteristic absorption peak at 652 nm increased upon introducing $H_2O_2$. As increasing concentration of $H_2O_2$, maximum absorbance intensity at 652 nm increased gradually. The relative absorbance intensity ($A - A_0$) is directly proportional to the concentration of $H_2O_2$ in range from 1 mM to 50 mM. The detection limit of $H_2O_2$ is 0.2 mM (S/N = 3). Compared with Fenton reaction, our proposed approach has comparable linear ranges for $H_2O_2$ detection (Fig. S1, ESI†). Thus, turn-on colorimetric determination of $H_2O_2$ is developed.

The BSA-Cu NPs-based colorimetric sensor is further applied to detect dopamine. Fig. 4B shows the absorption spectra of Cu NPs/TMB system in the presence of different amounts of analyte DA. The maximum absorbance intensity of the product of oxidized TMB at 652 nm decreased gradually with the increasing concentrations of DA (Fig. 4B), indicating that the absorbance intensity of the system was highly dependent on the concentration of DA. These situations confirm the feasibility of present BSA-Cu NPs as a colorimetric sensor of sensitively

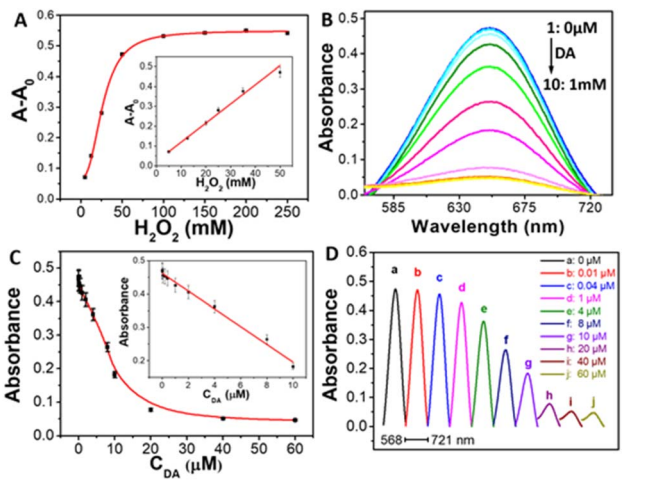


Fig. 4 (A) The curve of the absorbance intensity at 652 nm *versus* $H_2O_2$ concentration. Inset: the linear plot for $H_2O_2$ determination. (B) Absorption spectra of the TMB solution in the presence of various concentrations of DA by using BSA-Cu NPs as nanomaterial-based peroxidase mimics. (C) Plots of the absorbance intensity of TMB at 652 nm as a function of the concentration of the analyte DA. Inset: the linear calibration plot for DA detection. The error bars represent the standard deviation of three measurements. (D) Horizontal stacking diagram of UV-vis spectra of prepared BSA-Cu NPs incubated with different concentrations of target DA. Conditions: 1, (a), BSA-Cu NPs; 2–10 (b–j): 1 + DA (μM): 0.01, 0.04, 1, 4, 8, 10, 20, 40, and 60 μM, respectively.

sensing DA. Fig. 4C illustrated the graph between the absorption intensity at 652 nm and DA concentration. The maximum absorbance intensity exhibited a good linear relationship of DA concentration in the range from 10 nM to 10 μM (the inset of Fig. 4C). The linear regression equation is $A_0 - A = 0.46187 - 0.02666C_{DA}$ ($R = 0.9904$). The detection limit for analyzing DA is as low as 5 nM (S/N = 3). The detailed changes of absorbance intensity of TMB-$H_2O_2$-Cu NPs system incubated with different concentrations of target DA can be observed in Fig. 4D. Therefore, a novel turn-off colorimetric approach for detecting DA has been proposed.

### 3.6. Intelligent recognition of DA using synthesized BSA-Cu NPs nanozyme relying on smartphone-assisted analysis

In order to achieve a more simple and portable *in situ* detection, visual semi-quantitative test strip based on BSA-Cu NPs with the accurate color recognition function of smartphone has been designed and constructed. As shown in Fig. 5, the different concentrations lead to the change of distinguishable color. Besides, a series of test papers can be immediately captured by smartphone camera to ensure the accuracy of the method, linear relationship of DA quantitative detection is established with mean intensity as the ordinate and the concentration of DA as the abscissa (upper figure). There is good linear relationship, and linear regression equation is $Y = -10.04X + 158.83$ ($R^2 = 0.9981$), with the LOD of 0.05 μM, revealing that smartphone-assisted visual sensing approach can achieve efficient and sensitive detection of DA (lower figure).

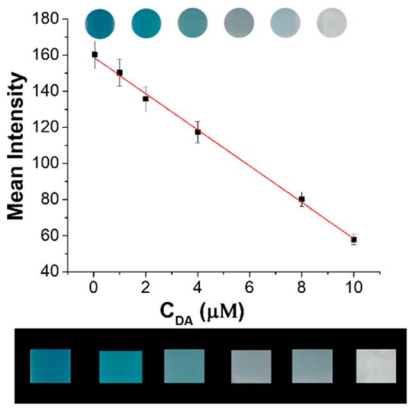


Fig. 5 The calibration curve of darkness density analyzed by image software Quantity One (upper figure). The photographs of DA intelligent recognition obtained by camera (lower figure). Conditions: concentrations of dopamine with BSA-Cu NPs nanozyme and TMB system (from the left to the right): 0, 1, 2, 4, 8, and 10 μM.

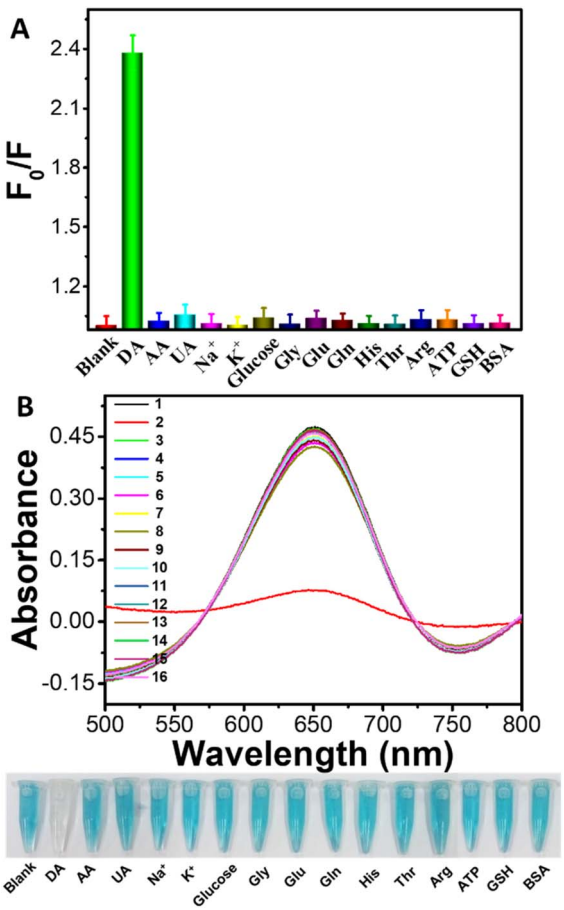


Fig. 6 The selectivity assays of fluorometric (A)/colorimetric (B) dual-mode monitoring of the analyte DA (20 μM) or other interferential substances (50 μM) based on BSA-Cu NPs nanozyme platform. Conditions: 1–16: blank, DA, AA (ascorbic acid), UA (uric acid), $Na^+$, $K^+$, glucose, Gly, Glu, Gln, His, Thr, Arg, ATP, GSH, and BSA. $F_0$ and $F$ are the emission intensity of synthesized BSA-Cu NPs without and incubated with DA or interferential substances, respectively. The error bars represent the standard deviation of three measurements.

Table 1 Comparison of analytical data of different methods for the detection of dopamine

| Method | Linear range (nM) | Detection limit (nM) | References |
|---|---|---|---|
| Electrochemistry detection | 5–1000 | 1 | 22 |
| Fluorescence detection | 10–20 000 | 1.8 | 23 |
| Fluorescence detection | 10–1000 | 10 | 24 |
| Colorimetric detection | 10–1000 | 10 | 24 |
| Colorimetric detection | 1000–10 000 | 109 | 25 |
| Fluorescence detection | 0.1–10 000 | 0.02 | 26 |
| BSA-Cu NCs-based fluorescence detection | 500–50 000 | 280 | 27 |
| BSA-Cu NPs-based fluorometric detection | 10–60 000 | 5 | This study |
| BSA-Cu NPs-based colorimetric detection | 10–10 000 | 5 | This study |

Table 2 Determination results of dopamine by using proposed fluorometric/colorimetric dual-mode approach based on BSA-Cu NPs nanozyme and HPLC approach in human serum samples

| | | Fluorometric approach | | | Colorimetric approach | | | HPLC method[b] | | |
|---|---|---|---|---|---|---|---|---|---|---|
| No. | Added (nM) | Measured[a] (nM) | R. S. D. ($n = 5\%$) | Recovery (%) | Measured[a] (nM) | R. S. D. ($n = 5\%$) | Recovery (%) | Measured[a] (nM) | R. S. D. ($n = 5\%$) | Recovery (%) |
| 1 | 200 | 196 ± 0.06 | 3.2 | 98 | 195 ± 0.08 | 3.3 | 97.5 | 197 ± 0.08 | 3.0 | 98.5 |
| 2 | 500 | 510 ± 0.12 | 5.5 | 102 | 512 ± 0.16 | 5.7 | 102.4 | 509 ± 0.13 | 5.2 | 101.8 |
| 3 | 800 | 824 ± 0.22 | 6.1 | 103 | 828 ± 0.30 | 6.3 | 103.5 | 826 ± 0.26 | 5.9 | 103.3 |

[a] Average values of five determinations ± standard deviation. [b] HPLC: high performance liquid chromatography.

On the whole, the experimental results suggest that BSA-Cu NCs is more suitable for determining DA than BSA-Au NCs. The detailed reasons are listed as follows: First, the synthesis of BSA-Cu NCs probe is more economical due to the price of raw materials which greatly expands their application scope. Second, maximum emission intensity of prepared BSA-Cu NCs in our assay has approximately 600 times variable interval while that of BSA-Au NCs only possesses 200 times. Third, the developed approach based on BSA-Cu NCs has lower sensitivity and wider linear range than that by using BSA-Au NCs regardless of fluorometric mode or colorimetric mode.[24] Moreover, a new smartphone-assisted analysis for DA detection on the basis of BSA-Cu NCs was also proposed. In addition, compared with other reported analytical methods, our present method possessed the comparable sensitivity and more wide linear ranges (Table 1).[22–27]

### 3.7. Anti-interference ability

To evaluate our present platform's selectivity, fluorometric/colorimetric responses of the TMB-$H_2O_2$-BSA-Cu NPs system to the interferential substances have been investigated. A series of possible coexisting substances including ascorbic acid (AA), uric acid (UA), carbohydrate, metal ions, amino acids, and protein are chosen and measured in our assays. As shown in Fig. 6A, introducing DA leads to drastical change in fluorescence intensity while adding interferential substances only induce slight changes. Similar conclusions are also obtained by colorimetric mode sensing approach (Fig. 6B). Moreover, absorbance changes induced by the addition of DA were clearly observed by naked eyes. The reactive solution containing DA was almost colorless while those including interferences displays a deep blue color, demonstrating high selectivity of this visual approach for DA determination (the lower photographs of Fig. 6B). The experimental results indicated that the present interferential substances has virtually no influence on the detection of DA and further demonstrated that BSA-Cu NPs-based fluorometric/colorimetric dual-channel sensing platform possessed quite high specificity for DA detection.

### 3.8. Analysis of actual samples

Finally, to further verify the actual detection performance of our developed nanozymes sensor, real human serum samples are tested by using standard addition method. The serum samples are diluted 100 times with PBS (pH 7.0) before the measurement. Experimental results obtained from proposed BSA-Cu NPs-based fluorometric/colorimetric dual-mode nanosensors are compared with those provided by traditional high performance liquid chromatography (HPLC) method. As displayed in Table 2, the detection results obtained by using both our fluorometric mode and the colorimetric mode are in good agreement with those obtained by using HPLC method. Besides, our developed method shows satisfactory recoveries ranging from 98% to 103% by fluorometric mode and from 97.5% to 103.5% by colorimetric mode. The results demonstrate that our proposed method is highly accurate and reliable for DA detection in actual samples. Therefore, our established fluorometric/colorimetric sensing platform possesses potential practical application in early diagnosis of diseases.

## 4. Conclusions

In conclusion, a label-free dual recognition strategy driven fluorometric/colorimetric dual-channel sensing platform for DA detection is developed by integrating the dual properties of fluorescence and catalysis of copper nanoparticles. In one fluorometric mode, the addition of DA induces drastical decrease of fluorescence intensity of BSA-Cu NPs located at 401 nm due to photo-induced electron transfer (PET) mechanism. In other colorimetric mode, as the as-fabricated BSA-Cu NPs exhibit high peroxidase-like activity, the introduction of DA can inhibit the catalytic activities of BSA-Cu NPs nanozyme, resulting in remarkable decrease of absorbance signal at 652 nm. Besides, by combining the test strips with smartphone-assisted analysis, an intelligent DA recognition on-site is also developed. Moreover, the developed dual-channel approach was successfully applied in the detection of dopamine in real samples. This work effectively expands the usage of boundary of fluorescent copper nanoparticles and will hold the good potential to be applied in bioanalysis and clinical diagnostics fields.

## Data availability

The datasets used and/or analyzed during the current study are available from the corresponding author on reasonable request.

## Author contributions

Da-Qian Feng: conceptualization, investigation, data curation. Shaofei Wang: validation. Zhendi Yu: validation. Wenfeng Zhang: validation. Guoliang Liu: supervision, writing-review & editing.

## Conflicts of interest

The author declare no conflict of interest.

## Acknowledgements

We are grateful for the financial support from the National Natural Science Foundation of China (No. 21501146), the Natural Science Foundation of Jiangsu Province (No. BK20150424 and BK20140464), and Postgraduate Research & Practice Innovation Program of Yancheng Institute of Technology (No. KYCX24_XZ017 and KYCX23_XY012).

## References

1 A. Desireddy, *et al.*, Ultrastable silver nanoparticles, *Nature*, 2013, **501**, 399–402.
2 M. J. Huang, *et al.*, Selective assemblies of giant tetrahedra via precisely controlled positional interactions, *Science*, 2015, **348**, 424–428.
3 Y. Chen, *et al.*, Multimodal plasmonic assay of copper(II) ion via stimuli-responsive state transformation of silver molecular nanoparticles, *Anal. Chem.*, 2016, **88**, 8123–8128.
4 Y. Tao, *et al.*, Metal nanoclusters: Novel probes for diagnostic and therapeutic applications, *Chem. Soc. Rev.*, 2015, **44**, 8636–8663.
5 L. B. Zhang and E. K. Wang, Metal nanoclusters: New fluorescent probes for sensors and bioimaging, *Nano Today*, 2014, **9**, 132–157.
6 G. L. Liu, *et al.*, Silver nanoclusters beacon as stimuli-responsive versatile platform for multiplex DNAs detection and aptamer-substrate complexes sensing, *Anal. Chem.*, 2017, **89**, 1002–1008.
7 M. Zhang, *et al.*, A label-free fluorescent molecular beacon based on DNA-templated silver nanoclusters for detection of adenosine and adenosine deaminase, *Chem. Commun.*, 2012, **48**, 5488–5490.
8 X. Hu, *et al.*, Recent advances in the analytical applications of copper nanoclusters, *TrAC Trend. Anal. Chem.*, 2016, **77**, 66–75.
9 Z. H. Qing, *et al.*, Poly(thymine)-templated selective formation of fluorescent copper nanoparticles, *Angew. Chem., Int. Ed.*, 2013, **52**, 9719–9722.
10 C. Wang, Y. G. Yao and Q. J. Song, Interfacial synthesis of polyethyleneimine-protected copper nanoclusters: Size-dependent tunable photoluminescence, pH sensor and bioimaging, *Colloids Surf., B*, 2016, **140**, 373–381.
11 N. Goswami, *et al.*, Copper quantum clusters in protein matrix: Potential sensor of $Pb^{2+}$ ion, *Anal. Chem.*, 2011, **83**, 9676–9680.
12 J. Y. Li, *et al.*, Fluorescence regulation of poly(thymine)-templated copper nanoparticles via an enzyme-triggered reaction toward sensitive and selective detection of alkaline phosphatase, *Anal. Chem.*, 2017, **89**, 3681–3686.
13 L. Z. Hu, *et al.*, Copper nanoclusters as peroxidase mimetics and their applications to $H_2O_2$ and glucose detection, *Anal. Chim. Acta*, 2013, **762**, 83–86.
14 Z. G. Mao, *et al.*, Poly(thymine)-templated copper nanoparticles as a fluorescent indicator for hydrogen peroxide and oxidase-based biosensing, *Anal. Chem.*, 2015, **87**, 7454–7460.
15 D. L. Robinson, *et al.*, Detecting subsecond dopamine release with fast-scan cyclic voltammetry in vivo, *Clin. Chem.*, 2003, **49**, 1763–1773.
16 A. Zhang, J. L. Neumeyer and R. J. Baldessarini, Recent progress in development of dopamine receptor subtype-selective agents: Potential therapeutics for neurological and psychiatric disorders, *Chem. Rev.*, 2007, **107**, 274–302.
17 G. W. She, *et al.*, $SnO_2$ nanoparticle-coated ZnO nanotube arrays for high-performance electrochemical sensors, *Small*, 2014, **10**, 4685–4692.
18 T. Kienast and A. Heinz, Dopamine and the diseased brain, *Drug Targets*, 2006, **5**, 109–131.
19 T. Qian, *et al.*, In situ polymerization of highly dispersed polypyrrole on reduced graphite oxide for dopamine detection, *Biosens. Bioelectron.*, 2013, **50**, 157–160.
20 J. R. Cooper, *et al.*, Patterns of loss of dopamine containing neurons in Parkinson's disease, *Brain*, 1999, **122**, 1437–1448.
21 F. J. Shang, *et al.*, Selective nanomolar detection of dopamine using a boron-doped diamond electrode modified with an electropolymerized sulfobutylether-beta-cyclodextrin-doped poly(*N*-acetyltyramine) and polypyrrole composite film, *Anal. Chem.*, 2009, **81**, 4089–4098.
22 H. Y. Tsai, Z. H. Lin and H. T. Chang, Tellurium-nanowire-coated glassy carbon electrodes for selective and sensitive detection of dopamine, *Biosens. Bioelectron.*, 2012, **35**, 479–483.
23 X. L. Zhang, *et al.*, A simple, fast and low-cost turn-on fluorescence method for dopamine detection using in situ reaction, *Anal. Chim. Acta*, 2016, **944**, 51–56.
24 Y. Tao, *et al.*, A dual fluorometric and colorimetric sensor for dopamine based on BSA-stabilized Au nanoclusters, *Biosens. Bioelectron.*, 2013, **42**, 41–46.
25 S. R. Ahmed, *et al.*, Target specific aptamer-induced self-assembly of fluorescent graphene quantum dots on palladium nanoparticles for sensitive detection of tetracycline in raw milk, *Food Chem.*, 2021, **346**, 128893.
26 H. B. Wang, *et al.*, A label-free and ultrasensitive fluorescent sensor for dopamine detection based on double-stranded DNA templated copper nanoparticles, *Sensor. Actuator. B Chem.*, 2015, **220**, 146–153.
27 Z. Miao, *et al.*, BSA capped bi-functional fluorescent Cu nanoclusters as pH sensor and selective detection of dopamine, *New J. Chem.*, 2018, **42**, 1446–1456.
28 D.-Q. Feng, *et al.*, Dual-modal light scattering and fluorometric detection of lead ion by stimuli-responsive

aggregation of BSA-stabilized copper nanoclusters, *RSC Adv.*, 2016, **6**, 96729–96734.

29 D.-Q. Feng and G. L. Liu, Target-activating and toehold displacement Ag NCs/GO biosensor-mediating signal shift and enhancement for simultaneous multiple detection, *Anal. Chem.*, 2021, **93**, 16025–16034.

30 D.-Q. Feng, *et al.*, Smart flared-nanokites with ultra-high fluorescence enhancement for multiplexing virus DNA biosensing, *Sensor. Actuator. B Chem.*, 2023, **387**, 133813.

31 G. L. Liu, *et al.*, Construction of FRET biosensor for off-on detection of lead ions based on carbon dots and gold nanorods, *Talanta*, 2019, **201**, 90–95.

32 W. J. Zhu, *et al.*, Bienzyme colorimetric detection of glucose with self-calibration based on tree-shaped paper strip, *Sensor. Actuator. B Chem.*, 2014, **220**, 414–418.

33 L. Shang, *et al.*, Recent advances in synthesizing metal nanocluster-based nanocomposites for application in sensing, imaging and catalysis, *Nano Today*, 2019, **28**, 100767.

34 Y. L. Xu, *et al.*, The role of protein characteristics in the formation and fluorescence of Au nanoclusters, *Nanoscale*, 2014, **6**, 1515–1524.

35 C. Wang, *et al.*, Protein-directed synthesis of pH-responsive red fluorescent copper nanoclusters and their applications in cellular imaging and catalysis, *Nanoscale*, 2014, **6**, 1775–1781.

36 X. Y. Yue, *et al.*, A portable smartphone-assisted ratiometric fluorescence sensor for intelligent and visual detection of malachite green, *Food Chem.*, 2022, **371**, 131164.

37 P. Ray and A. J. Steckl, Label-free optical detection of multiple biomarkers in sweat, plasma, urine, and saliva, *ACS Sens.*, 2019, **4**, 1346–1357.

38 F. Zu, *et al.*, The quenching of the fluorescence of carbon dots: A review on mechanisms and applications, *Microchim. Acta*, 2017, **184**, 1899–1914.

39 Y. Li, *et al.*, Investigation of photo-induced electron transfer between amino-functionalized graphene quantum dots and selenium nanoparticle and it's application for sensitive fluorescent detection of copper ions, *Talanta*, 2019, **197**, 341–347.

40 J. Y. Zhang, *et al.*, Optically-active nanocrystals for inner filter effect-based fluorescence sensing: Achieving better spectral overlap, *TrAC Trend. Anal. Chem.*, 2019, **110**, 183–190.

41 L. Z. Hu, *et al.*, Copper nanoclusters as peroxidase mimetics and their applications to $H_2O_2$ and glucose detection, *Anal. Chim. Acta*, 2013, **762**, 83–86.

42 H. L. Tan, *et al.*, Metal-organic framework-derived copper nanoparticle@carbon nanocomposites as peroxidase mimics for colorimetric sensing of ascorbic acid, *Chem. Eur. J.*, 2014, **20**, 16377–16383.